



**EXPLAINABLE SELF-SUPERVISED LEARNING TO PREDICT AND GENERATE  
NUTRIENT CANAL DIAMETERS FROM MANDIBULAR CONE-BEAM  
COMPUTED TOMOGRAPHY ANALYSIS**

**Amit Rajabhau Pawar<sup>1</sup>, Pradeep Kumar Yadalam<sup>2</sup>, Gurumoorthy  
Kaarthikeyan<sup>3</sup>, Carlos M. Ardila<sup>4</sup>**

1. Department of Periodontics, Saveetha Dental College and Hospitals, Saveetha Institute of Medical and Technical Sciences (SIMATS), Saveetha University, Chennai, Tamil Nadu, India.
2. Department of Periodontics, Saveetha Dental College and Hospitals, Saveetha Institute of Medical and Technical Sciences (SIMATS), Saveetha University, Chennai, Tamil Nadu, India.
3. Department of Periodontics, Saveetha Dental College and Hospitals, Saveetha Institute of Medical and Technical Sciences (SIMATS), Saveetha University, Chennai, Tamil Nadu, India..
4. Department of Basic Sciences, Biomedical Stomatology Research Group, Faculty of Dentistry, Universidad de Antioquia U. de A., Medellín, Colombia.

Received: 23/12/2024

Accepted: 21/01/2025

**EMAIL:** [martin.ardila@udea.edu.co](mailto:martin.ardila@udea.edu.co) / [pradeepkumar.sdc@saveetha.com](mailto:pradeepkumar.sdc@saveetha.com)



## ABSTRACT

**Introduction:** Cone-beam computed tomography (CBCT) has revolutionized dentistry by providing high-resolution 3D views for evaluating mandibular nutrient canal systems. However, manual measurements are time-consuming. This study employs self-supervised learning to predict nutrient canal measurements from mandibular CBCT scans. **Objective:** To enhance accuracy and treatment planning using explainable artificial intelligence (AI), optimizing strategies for implant surgeries and personalized care. **Methods:** A total of 398 CBCT images were collected from the DIAS system at Saveetha Dental College. A periodontist annotated data, including nutrient canal diameter, lingual artery visibility, and distances. Data were split into training and testing sets. The self-supervised model utilized autoencoders with encoder, decoder, and regression heads, compressing data into a 16-dimensional latent space to predict canal diameter. **Results:** The model reduced reconstruction and regression losses, achieving final losses of 0.2543 for reconstruction and 0.3336 for regression. **Conclusion:** Self-supervised learning can enhance CBCT scan analysis by predicting canal diameters. However, success depends on high-quality data, robust validation, and multimodal integration.

**KEYWORDS:** Cone Beam Computed Tomography; dentistry; high-resolution; three-dimensional views; dental anatomy; nutrient canal systems; machine learning.



## APRENDIZAJE AUTO-SUPERVISADO EXPLICABLE PARA PREDECIR Y GENERAR LOS DIÁMETROS DE CANALES NUTRICIOS EN TOMOGRAFÍA COMPUTARIZADA DE HAZ CÓNICO

### RESUMEN

**Introducción:** La tomografía computarizada de haz cónico (CBCT) ha transformado la odontología al proporcionar vistas tridimensionales de alta resolución para evaluar los sistemas de canales nutricios mandibulares. Sin embargo, las mediciones manuales son laboriosas. Este estudio utiliza aprendizaje auto-supervisado para predecir mediciones de los canales nutricios a partir de escaneos CBCT mandibulares. **Objetivo:** Mejorar la precisión y la planificación del tratamiento mediante inteligencia artificial explicable (IA), optimizando estrategias para cirugías de implantes y atención personalizada. **Métodos:** Se recopilieron 398 imágenes CBCT del sistema DIAS del Saveetha Dental College. Un periodoncista calificó los datos, incluyendo mediciones del diámetro del canal nutricional, visibilidad de la arteria lingual y distancia. Los datos se dividieron en conjuntos de entrenamiento y prueba. El modelo auto-supervisado empleó autoencoders con codificador, decodificador y cabeza de regresión, comprimiendo los datos en un espacio latente de 16 dimensiones para predecir el diámetro del canal. **Resultados:** El modelo redujo pérdidas de reconstrucción y regresión, logrando una pérdida final de 0.2543 para reconstrucción y 0.3336 para regresión. **Conclusión:** El aprendizaje auto-supervisado puede mejorar el



análisis de escaneos CBCT al predecir diámetros de los canales, aunque su éxito depende de datos de alta calidad, validación robusta e integración multimodal.

**PALABRAS CLAVE:** Tomografía computarizada de haz cónico; odontología; alta resolución; vistas tridimensionales; anatomía dental; sistemas de canales nutricios; aprendizaje automático.

## INTRODUCTION

Cone Beam Computed Tomography (CBCT) has emerged as a revolutionary imaging modality in dentistry, offering high-resolution three-dimensional views of dental anatomy (1). This advanced imaging technique allows for a more detailed evaluation of the nutrient canal system than traditional two-dimensional radiographs, providing critical insights into nutrient canal dimensions. CBCT offers advantages, but manual canal diameter measurement is labor-intensive.

Advances in dental imaging are enhancing accuracy using machine learning algorithms, leading to improved implant planning and personalized interventions (2).

A previous study of 194 patients found nutrient canals in 94.3% of cases, mainly in the front area, with an average of 2.7 canals and 1.0 mm diameter. Understanding these canals can prevent dental procedures (3). A study on 50 CBCT scans of the mandible found 243 accessory canals and 245 accessory



foramina, with males having a higher prevalence (53%). Most were located in the anterior region, with females having more accessory canals and foramina (4). These studies have shown the presence and diameter of nutrient canals, but their prediction of the diameter of nutrient canals has not been analyzed much.

CBCT is crucial for predicting nutrient canals, which carry blood vessels and nerves, enabling better treatment planning and influencing surgical outcomes, especially in complex cases like implants and extractions (5). Predictive models for nutrient canals enable practitioners to tailor their surgical approaches, improving overall treatment outcomes. Recent work on 104 patients found discrepancies in mandibular canal localization accuracy between three

experienced clinicians and five tracings. The posterior and anterior loops had higher mean RMS error experienced clinicians who take longer to trace canal localizations than AI-driven segmentation, indicating that clinician experience significantly influences accuracy (6).

AI-driven segmentation is time-efficient but requires verification to avoid errors similar to this study's accuracy. These studies have identified the mandibular canal's location but have not determined the nutrient canal's diameter (7). So, we used the supervised learning method to predict and generate the nutrient canal dimensions in mandibular CBCT. Recent advancements in self-supervised learning and deep learning methodologies present exciting opportunities to improve the



modeling of complex patterns in dental images. These innovative techniques can leverage vast amounts of unlabeled data from CBCT scans (8) to develop robust predictive models that learn to identify significant features associated with canal dimensions. This study chose self-supervised learning for nutrient canal prediction and generation due to its ability to utilize unlabeled data effectively, enhancing the model's ability to discern complex patterns, especially in the intricate nature of nutrient canal generation (9). By accurately predicting canal diameters using AI, practitioners

can better understand the nutrient canal system, optimize treatment strategies, and ultimately enhance patient care. This study explores the effectiveness of self-supervised learning methods in predicting dental canal diameters from CBCT images, aiming to improve accuracy and decision-making with explainable AI.

### **Materials and Methods**

Figure 1 shows the workflow of the nutrient canal diameter.

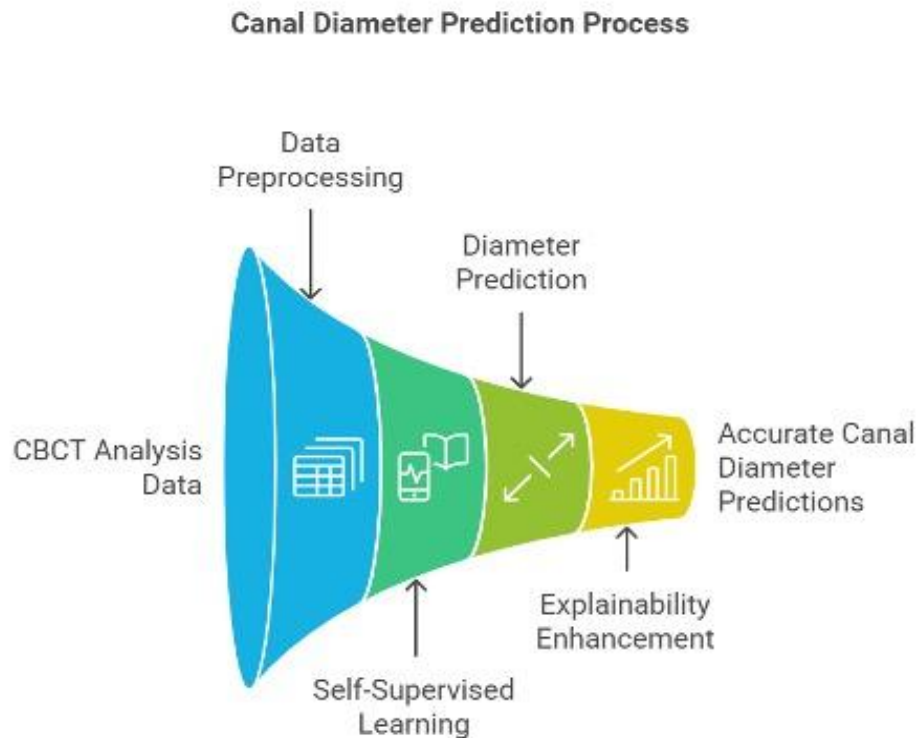


**Figure 1.** Workflow of the nutrient canal diameter.

### Data Preparation

The dataset for this study was obtained from Saveetha Dental College utilizing the DIAS information system. A total of 398 images with their data were collected from cone beam computed tomography

(CBCT) images, which included essential demographic details such as age and gender and information regarding the presence and characteristics of nutrient canals. Specifically, the dataset encompassed measurements including the diameter of the canals, visibility of the



lingual artery, and the distances from the lingual artery to the inferior border (in millimeters). A qualified periodontist meticulously obtained these measurements, and a data frame was subsequently prepared based on this comprehensive dataset (Figure 1).

### Data preprocessing

The study normalizes nine input features using an 80-20 train-test split and a 32-batch batch size. Preprocessing of the data includes removing duplicates and missing values.

### Self-supervised learning architecture

The self-supervised approach combines unsupervised feature learning with supervised regression (10, 11), allowing

the model to learn meaningful representations while maintaining predictive accuracy for nutrient canal diameter estimation. The architecture details include a sequenced encoder, a linear decoder, and a linear regression. The training configuration includes an optimizer, a learning rate of 0.001, 100 epochs, 32 batch sizes, and weight initialization by Xavier/Glorot. The model is designed to reconstruct input data and predict a specific target variable, such as nutrient canal dieter. The model's architecture includes a custom `Autoencoder` class, compressing the input data into a lower-dimensional representation using ReLU activation functions. The decoder reconstructs the original input from the latent representation using ReLU activations.





The regressor is a regression head that predicts the target variable using two linear layers. A forward pass method passes a tensor  $x$  as input, obtains the encoded representation, and generates the reconstructed output. An Adam optimizer is initialized to optimize model parameters with a learning rate of 0.001.

The self-supervised model is an autoencoder-based architecture with three main components:

**Encoder:** Compresses the input data into a 16-dimensional latent space using fully connected layers ( $64 \rightarrow 32 \rightarrow 16$  neurons) with ReLU activations.

**Decoder:** Reconstructs the input data from the latent space using a mirrored structure ( $16 \rightarrow 32 \rightarrow 64 \rightarrow 9$  neurons). **Regression Head:** A single

linear layer ( $16 \rightarrow 1$ ) predicts the nutrient canal diameter from the latent representation.

The architecture ensures that the encoder learns meaningful representations while simultaneously predicting the target variable.

### Training Objectives

The model was trained with two objectives: reconstruction loss (measured using Mean Squared Error) and regression loss (measured using MSE), with the total loss being a weighted sum of these components.

### Input Data Format

The input data consisted of 9 features, including demographic, anatomical, and



clinical variables. These features were normalized to ensure consistent scaling. The target variable was the nutrient canal diameter, a continuous variable.

The proposed model uses a structured architecture with an encoder, decoder network, and a regression head to predict nutrient canal diameter from a latent representation. The encoder network compresses input data into a 16-dimensional latent space, while the decoder network mirrors the encoder structure, extending the latent representation to the original nine features. ReLU activations are applied between the decoder layers to maintain nonlinear transformations. The model is trained for 100 epochs, with a summary output printed every 10. The training process follows a systematic approach,

beginning with data preparation that includes normalization of the nine input features. The dataset is split into training and test sets, with an 80-20 ratio (320 training samples and 80 testing samples), and a batch size of 32 is employed during training. For optimization, the Adam optimizer is selected with a learning rate of 0.001, and the model is trained over 100 epochs. Weight initialization is carried out using the Xavier/Glorot method, ensuring appropriate weight distribution at the start of training. The forward pass involves data processing through an encoder, decoder, and regressor, combining reconstruction and regression losses to derive a total loss.

In contrast, the backward pass computes gradients for model parameter updates. The self-supervised approach combines



unsupervised feature learning with supervised regression to estimate nutrient canal diameter accurately. The model summary provides a comprehensive overview of layers, training configurations, optimizer, learning rate, epochs, batch size, and weight initialization method.

Comparison with SOTA- deep neural networks.

The SOTA (State-Of-The-Art) model is a deep neural network comprising three hidden layers with sizes 64, 32, and 16. It uses ReLU activation functions and concludes with a regression layer. The model was trained over 100 epochs using the Adam optimizer.

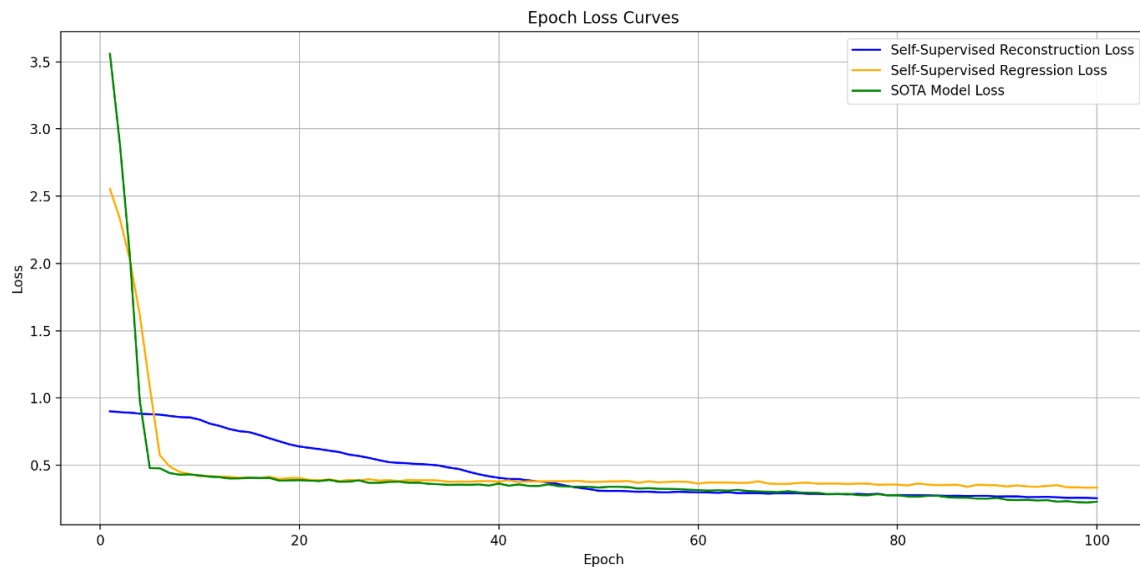
## Results

The self-supervised model has improved performance, reduced reconstruction and regression losses, and resulted in acceptable test losses. The test losses are recorded as a Test Reconstruction Loss of 0.2291 and a Test Regression Loss of 0.3135. The evaluation metrics included an R-squared of 0.2138, a mean absolute error of 0.4454, and a root mean squared error of 0.5599. The reconstruction objective aims to assess the fidelity of the input reconstruction through Mean Squared Error (MSE) loss, achieving a final reconstruction loss of 0.2543. This objective ensures meaningful feature extraction, allowing the model to learn compact and relevant representations of the input data.



Meanwhile, the regression objective is centered on predicting the nutrient canal diameter, also utilizing MSE loss, with a final regression loss calculated at 0.3336. After evaluating and comparing this model with a self-supervised model, the results indicate that the SOTA deep neural network model showed comparable results with a test loss of 0.2409 compared to 0.3135. Both models show a good correlation between predicted and actual values, as the scatter plots illustrate.

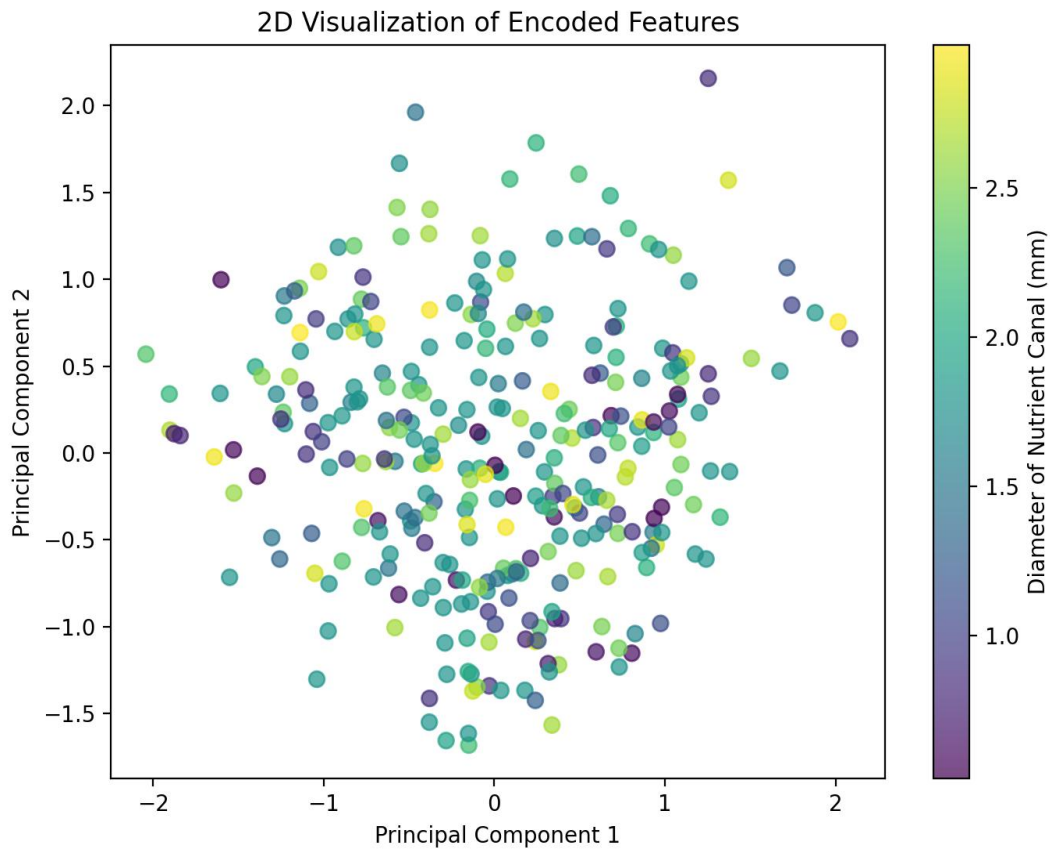
Figure 2 shows epoch loss curves for three metrics over 100 training epochs. The self-supervised reconstruction loss, self-supervised regression loss, and SOTA model loss all decrease over epochs, indicating successful learning and adaptation of the model. The convergence of the curves around low loss values (0.5) suggests effective performance across self-supervised tasks and the SOTA model. Overall, the training process has been successful, with a notable reduction in loss values.



**Figure 2.** Epoch loss curves for three metrics over 100 training epochs.

Figure 3 shows a scatter plot showing a 2D visualization of encoded features, likely derived from Principal Component Analysis (PCA). It includes axes representing Principal Components 1 and 2 and data points representing observations. The data is analyzed using Principal Components 1 (PC1) and 2 (PC2), linear combinations of original

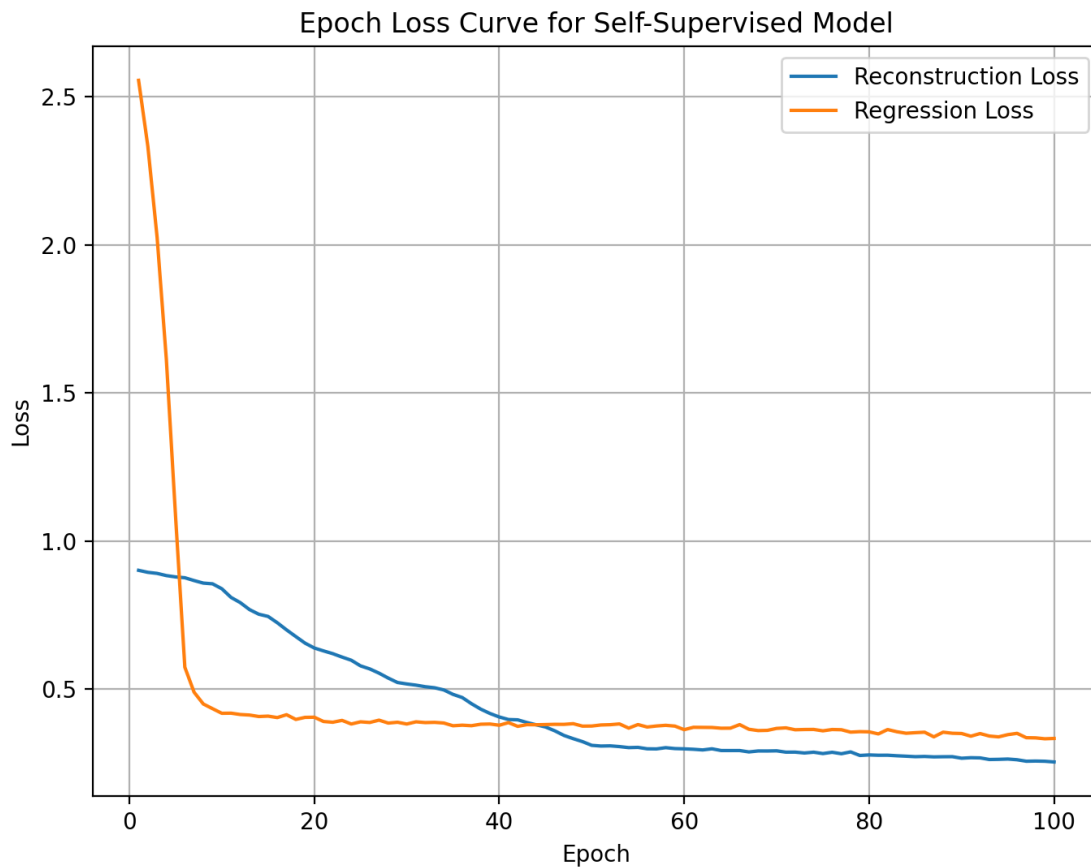
features. The points represent data samples in a 2D space, with color gradients corresponding to diameters. The data is not separable, but subtle patterns or trends may exist. PC1 and PC2 explain the most variance in the data, while the color gradient suggests a relationship with the diameter.



**Figure 3.** Scatter plot showing a 2D visualization of encoded features.

Figure 4 shows a self-supervised model's loss curve over 100 epochs, showing Reconstruction and Regression losses. The graph shows a successful training

process with a high initial spike, a rapid drop in losses after 20 epochs, and minimal improvements by the end.



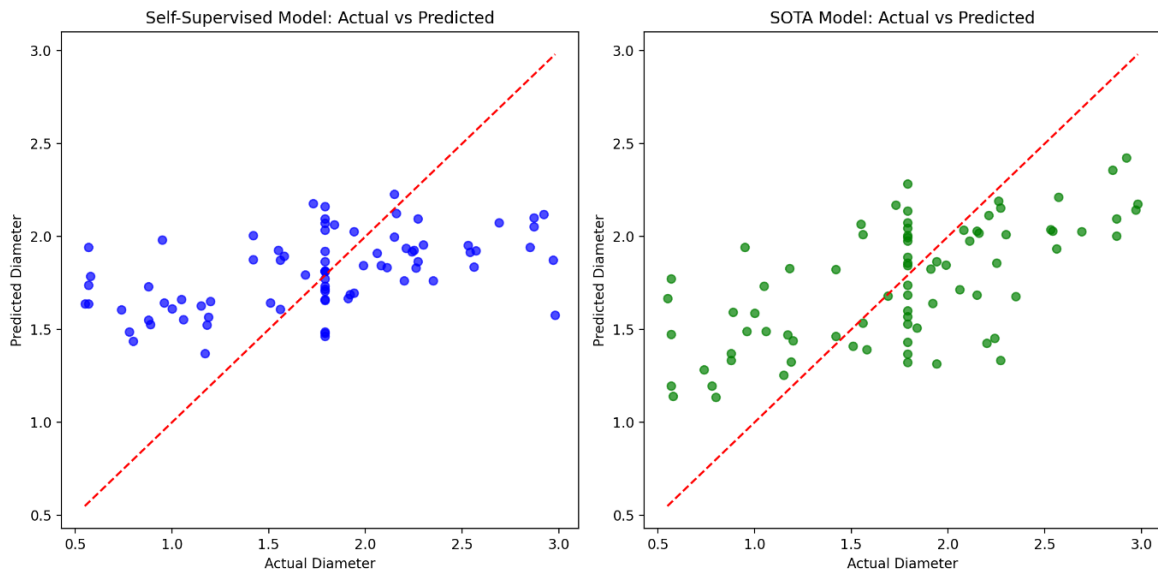
**Figure 4.** Self-supervised model's loss curve over 100 epochs.

Figure 5 shows scatter plots comparing actual and predicted diameters for self-supervised and state-of-the-art (SOTA) models. The self-supervised model shows variability and under-prediction, while the

SOTA model aligns better with actual values. Both models show some alignment with actual measurements, but the SOTA model demonstrates comparable predictive accuracy. The self-

supervised model's spread of points indicates variability and potential underestimation and Mean Squared Error (MSE) loss function, resulting in a final training loss of 0.2290, reflecting effective learning. Additional evaluation

metrics for the self-supervised model were provided: R-squared at 0.2138, Mean Absolute Error (MAE) at 0.4454, and Root Mean Squared Error (RMSE) at 0.5599, indicating moderate predictive ability.



**Figure 5.** Scatter plots comparing actual and predicted diameters for self-supervised and state-of-the-art (SOTA) models.





## Explainable AI-SHAP ANALYSIS

The feature importance analysis revealed three key attributes significantly influencing the models' predictions. The feature 'Gender\_encoded' scored highest at '0.253', indicating its significant role in determining the target variable. The predictive model identifies the number of nutrient canals as a key factor with an importance score of 0.238, indicating its relevance in solving the problem. The feature 'Presence\_encoded' was given a score of '0.221', indicating its significant role in the model's decision-making process. The study found a weak but positive correlation between visibility and location features and the target variable, with visibility\_encoded showing the highest correlation at 0.076.

Table 1 shows the dataset's shap plot-correlation analysis revealed a linear relationship between various features and the target variable. Visibility\_encoded showed the highest positive correlation with the target variable at 0.0756, suggesting a slight positive relationship. The number of nutrient canals and distance from the lingual artery to the inferior border had moderate positive correlations. Gender\_encoded had a minimal positive correlation, while age and distance from the lingual artery showed negligible or negative correlations. The location\_encoded feature had a slight negative correlation, suggesting it may contribute less to predicting the target variable. The model's encoder weights were used to assess the importance of three key features:



Gender\_encoded, Number of Nutrient Canals, and Presence\_encoded. Visibility\_encoded had the highest correlation with the target variable, while Region\_encoded had the lowest. These features were identified as the top three influential ones.

## Discussion

CBCT imaging facilitates detailed assessment and diagnosis of pathologies related to nutrient canals, such as infections or cysts. The CBCT-based identification of nutrient canal diameters in the mandible offers significant clinical benefits in dental practice. It allows for more precise implant surgical planning, reducing the risk of intraoperative complications and enhancing patient

outcomes. Accurate prediction of nutrient canals also aids in effectively administering local anesthesia, improving patient comfort and reducing anxiety. The diameter of nutrient canals can provide valuable insights into the health and density of the surrounding bone tissue, which can be critical when assessing candidates for dental implants or other surgical interventions (12).

Understanding nutrient canals' diameter and condition helps clinicians select implant types and techniques, plan bone augmentation procedures, and avoid canals during grafting to preserve vascular supply and enhance healing (8,13). Preoperative CBCT imaging allows for a more accurate surgical guide design tailored to the patient's unique anatomy, leading to improved clinical



outcomes and a higher implant success rate. In cases where immediate implant placement is considered post-extraction, awareness of nutrient canals is essential to avoid potential complications. CBCT helps in personalized treatment plans for implant patients, enhancing the surgical experience, maximizing implant success, and ensuring bone health and patient satisfaction.

One study analyzing mandibular CT images of 194 patients found that nutrient canals were present in 94.3% of the mandible, primarily in the anterior region. The study found that the most common nutrient canal length in Chennai patients was 6-10 mm (54.55%), with higher prevalence in males (58%), and the highest prevalence in the age group of 41-60 years (51%). No significant

associations were found between age and nutrient canal measurements. The canals were particularly visible between the central and lateral incisors (2). Understanding the position and anatomy of mandibular nutrient canals can help prevent complications, as 80% of cases have ovoid foramina between incisors (3).

A previous study categorized 200 CBCT scans into training, validation, and test sets. Oral radiologists manually segmented the scans in multiplanar reconstructions. Intra- and interobserver analysis was performed on 20% of the data set. Segments were then imported into Mimics for standardization (14). The study concludes that an innovative AI tool for automated segmentation of mandibular incisive canal on CBCT scans is accurate, time-efficient, and highly



consistent. Similar to this study, results with a self-supervised model have shown improved performance, reduced reconstruction and regression losses, and acceptable test losses. The model achieved a Test Reconstruction Loss of 0.2291 and a Test Regression Loss of 0.3135, with acceptable metrics. The reconstruction objective assessed the fidelity of the input reconstruction using Mean Squared Error (MSE) loss, achieving a final loss of 0.2543. The regression objective predicted the nutrient canal diameter using MSE loss, achieving a final loss of 0.3336. The SOTA model demonstrated effective learning with a final training loss of 0.2290, outperforming a self-supervised model with a regression loss of 0.3135. The self-supervised model had moderate

predictive ability, with R-squared at 0.2138, MAE at 0.4454, and RMSE at 0.5599 (Figures 2-5 and Table 1).

Self-supervised learning (15–17) has shown promise in predicting canal diameters in mandibular CBCT scans, but there are limitations to its effectiveness. These include reliance on labeled data, limited generalization, complexity in model interpretability, variability of measurements, and overfitting risks. Advanced model architectures, data augmentation techniques, and multi-modal data integration can improve predictive accuracy and generalization (10, 11, 18). Fine-tuning with supervised learning on a smaller labeled dataset can yield better performance and stronger predictive capabilities. Feature optimization through interpretability tools



can refine feature selection and improve interpretability. Robust validation techniques like k-fold cross-validation or bootstrapping can assess the model's robustness and ensure its reliability across different datasets. Real-time prediction systems can enhance practitioners' decision-making processes, translating into better patient care (9). However, self-supervised learning faces limitations such as dependency on labeled data, limited generalization, feature misrepresentation, complexity in model interpretability, data quality concerns, variability of nutrient canal measurements across practitioners, and overfitting risks.

## Conclusion

Self-supervised learning can revolutionize mandibular CBCT scan analysis, especially in predicting nutrient canal diameters. These models can uncover hidden patterns using unlabeled data and advanced neural network architectures. Hybrid learning, real-time prediction systems, and improved model interpretability are crucial for bridging the algorithm-clinical gap, but addressing limitations like generalization, interpretation complexity, and data quality is essential.

## Conflict of Interest

The authors have no conflicts of interest to declare

## Authors contribution



**Conceptualization:** Amit Rajabhau Pawar, Pradeep Kumar Yadalam, Gurumoorthy and Carlos M. Ardila. **Methodology:** Amit Rajabhau Pawar, Pradeep Kumar Yadalam, Gurumoorthy and Carlos M. Ardila. **Software:** Pradeep Kumar Yadalam. **Formal analysis:** Amit Rajabhau Pawar, Pradeep Kumar Yadalam, Gurumoorthy and Carlos M. Ardila. **Investigation,** Amit Rajabhau Pawar, Pradeep Kumar Yadalam, Gurumoorthy and Carlos M. Ardila. **Data curation:** Amit Rajabhau Pawar, Pradeep Kumar Yadalam, Gurumoorthy and Carlos M. Ardila. **Writing-original draft preparation,** Pradeep Kumar Yadalam and Carlos M. Ardila; **writing-review and editing,** Pradeep Kumar Yadalam and Carlos M. Ardila; **administration:** Pradeep Kumar Yadalam

**Ethics approval:** Not applicable

## REFERENCES

1. Alshomrani F. Cone-Beam Computed Tomography (CBCT)-Based Diagnosis of Dental Bone Defects. *Diagnostics* (Basel). 2024;14(13):1404
2. Patel JR, Wuehrmann AH. A radiographic study of nutrient canals. *Oral Surg Oral Med Oral Pathol.* 1976;42(5):693-701.
3. Kawashima Y, Sekiya K, Sasaki Y, Tsukioka T, Muramatsu T, Kaneda T. Computed Tomography Findings of Mandibular Nutrient Canals. *Implant Dent.* 2015;24(4):458–63.
4. Muley P, Kale L, Choudhary S, Aldhuwayhi S, Thakare A, Mallineni SK. Assessment of Accessory Canals and Foramina in the Mandibular Arch Using Cone-Beam Computed



Tomography and a New Classification for Mandibular Accessory Canals.

Biomed Res Int. 2022;2022:5542030.

5. Ogawa A, Fukuta Y, Nakasato H, Nakasato S. Cone beam computed tomographic evaluation of nutrient canals and foramina in the anterior region of the mandible. *Surg Radiol Anat.* 2016 ;38(9):1029–32.

6. Di Bartolomeo M, Pellacani A, Bolelli F, Cipriano M, Lumetti L, Negrello S, et al. Inferior Alveolar Canal Automatic Detection with Deep Learning CNNs on CBCTs: Development of a Novel Model and Release of Open-Source Dataset and Algorithm. *Appl. Sci.* 2023;13(5):3271

7. Park CS, Kang SR, Kim JE, Huh KH, Lee SS, Heo MS, et al. Validation of bone mineral density measurement using quantitative CBCT image based on deep learning. *Sci Rep.* 2023;13(1):11921.

8. Fan W, Zhang J, Wang N, Li J, Hu L. The Application of Deep Learning

on CBCT in Dentistry. *Diagnostics (Basel).* 2023;13(12):2056

9. Chen L, Liang X, Shen C, Nguyen D, Jiang S, Wang J. Synthetic CT generation from CBCT images via unsupervised deep learning. *Phys Med Biol.* 2021;66(11).

10. Yan K, Cai J, Jin D, Miao S, Guo D, Harrison AP, et al. SAM: Self-Supervised Learning of Pixel-Wise Anatomical Embeddings in Radiological Images. *IEEE Trans Med Imaging.* 2022;41(10):2658–69.

11. Ghesu FC, Georgescu B, Mansoor A, Yoo Y, Neumann D, Patel P, et al. Contrastive self-supervised learning from 100 million medical images with optional supervision. *J Med Imaging (Bellingham).* 2022;9(6):64503.

12. Zhi S, Kachelrieß M, Mou X. Spatiotemporal structure-aware dictionary learning-based 4D CBCT reconstruction. *Med Phys.* 2021;48(10):6421–36.

13. Tumer H, Orhan K, Aksoy S, Berberoglu A. Cone-beam-computed tomography evaluation of mandibular



nutrient canals in patients with periodontal diseases. Niger J Clin Pract. 2023 ;26(1):59–64.

14. Jindanil T, Marinho-Vieira LE, de-Azevedo-Vaz SL, Jacobs R. A unique artificial intelligence-based tool for automated CBCT segmentation of mandibular incisive canal. Dentomaxillofac Radiol. 2023;52(8):20230321.

15. Gong R, Wang L, Wang J, Ge B, Yu H, Shi J. Self-Distilled Supervised Contrastive Learning for diagnosis of breast cancers with histopathological images. Comput Biol Med. 2022;146:105641.

16. Li G, Togo R, Ogawa T, Haseyama M. Self-supervised learning for gastritis detection with gastric X-ray images. Int J Comput Assist Radiol Surg. 2023;18(10):1841–8.

17. Anand D, Annangi P, Sudhakar P. Benchmarking Self-Supervised Representation Learning from a million Cardiac Ultrasound images. Annu Int Conf IEEE Eng Med Biol Soc. 2022;2022:529–32.

18. Li G, Togo R, Ogawa T, Haseyama M. COVID-19 detection based on self-supervised transfer learning using chest X-ray images. Int J Comput Assist Radiol Surg. 2023 ;18(4):715–22.